www.nature.com/aps

Acta Pharmacologica Sinica

ARTICLE

PXR mediates mifepristone-induced hepatomegaly in mice

Xin-peng Yao[1], Ting-ying Jiao[1], Yi-ming Jiang[1], Shi-cheng Fan[1], Ying-yuan Zhao[1], Xiao Yang[1], Yue Gao[1], Fei Li[2], Yan-ying Zhou[1], Pan-pan Chen[1], Min Huang[1] and Hui-chang Bi[1,3]

Mifepristone (Mif), an effective synthetic steroidal antiprogesterone drug, is widely used for medical abortion and pregnancy prevention. Due to its anti-glucocorticoid effect, high-dose Mif is also used to treat Cushing's syndrome. Mif was reported to active pregnane X receptor (PXR) in vitro and PXR can induce hepatomegaly via activation and interaction with yes-associated protein (YAP) pathway. High-dose Mif was reported to induce hepatomegaly in rats and mice, but the underlying mechanism remains unclear. Here, the role of PXR was studied in Mif-induced hepatomegaly in C57BL/6 mice and *Pxr*-knockout mice. The results demonstrated that high-dose Mif (100 $mg \cdot kg^{-1} \cdot d^{-1}$, *i.p.*) treatment for 5 days significantly induced hepatomegaly with enlarged hepatocytes and promoted proliferation, but low dose of Mif (5 $mg \cdot kg^{-1} \cdot d^{-1}$, *i.p.*) cannot induce hepatomegaly. The dual-luciferase reporter gene assays showed that Mif can activate human PXR in a concentration-dependent manner. In addition, Mif could promote nuclear translocation of PXR and YAP, and significantly induced the expression of PXR, YAP, and their target proteins such as CYP3A11, CYP2B10, UGT1A1, ANKRD, and CTGF. However, Mif (100 $mg \cdot kg^{-1} \cdot d^{-1}$, *i.p.*) failed to induce hepatomegaly in *Pxr*-knockout mice, as well as hepatocyte enlargement and proliferation, further indicating that Mif-induced hepatomegaly is PXR-dependent. In summary, this study demonstrated that PXR-mediated Mif-induced hepatomegaly in mice probably via activation of YAP pathway. This study provides new insights in Mif-induced hepatomegaly, and provides novel evidence on the crucial function of PXR in liver enlargement and regeneration.

Keywords: mifepristone; hepatomegaly; pregnane X receptor (PXR); yes-associated protein (YAP)

Acta Pharmacologica Sinica (2022) 43:146–156; https://doi.org/10.1038/s41401-021-00633-4

INTRODUCTION

Mifepristone (Mif), which exerts its pharmacological effect mainly by antagonizing progesterone receptor, is often used for early pregnancy termination, pregnancy prevention, and endometrial cancer at normal low dose of 25–150 mg/d [1–3]. High-dose Mif was found to have an anti-glucocorticoid effect [4]. In 2012, FDA approved high-dose Mif (300–1200 mg/d) for the treatment of abnormal elevation of serum glucocorticoid caused by primary or secondary adrenal tumors, which is called the Cushing's syndrome (CS) [5]. Mif was also known to activate both human pregnane X receptor (hPXR) and mice PXR (mPXR) in vitro [6]. A significant increase in liver weight was observed after treatment of high-dose Mif at 200 $mg \cdot kg^{-1} \cdot d^{-1}$ in rats and 100 $mg \cdot kg^{-1} \cdot d^{-1}$ in mice [7, 8]. Most recently, we found that treatment of 100 $mg \cdot kg^{-1} \cdot d^{-1}$ Mif for 5 days induced significant hepatomegaly in mice. However, the underlying mechanism of Mif-induced hepatomegaly remains unknown.

Hepatomegaly, which is also called liver enlargement, liver hypertrophy, or liver hyperplasia, is a clinical symptom caused by numerous factors, such as hepatic enzymes induction, injuries, infections, or carcinogenicities [9]. The manifestations of hepatomegaly include hepatocyte hyperplasia or hepatocellular hypertrophy. Hepatomegaly can be classified into adverse hepatomegaly or non-adverse hepatomegaly (the latter one is also called adaptive or benign hepatomegaly). Hepatomegaly without hepatoxicity evidenced by increased serum biochemical parameters or morphological changes is considered as a non-adverse hepatomegaly, which is commonly induced by drugs and will disappear after withdrawal [9, 10]. Nuclear receptors (NRs), which play an important role in metabolism of drugs and endogenous molecules, are widely distributed in liver and their activation is considered to be closely related to hepatomegaly [9, 11]. For example, constitutive androstane receptor (CAR) has been reported to be the critical factor of hepatomegaly induced by barbiturates [12]. And it has been reported that the activation of peroxisome proliferator-activated receptor α (PPARα) could induce hepatomegaly [13].

PXR, a member of NR superfamily, is mainly distributed in liver and intestine with a wide range of functions. As PXR plays a pivotal role in xenobiotics detoxification and energy metabolism, it is closely related to the physiology and pathology of liver [14]. Pregnenolone-16α-carbonitrile (PCN), a mouse-specific PXR agonist, can significantly induce liver hyperplasia and hypertrophy [15]. The PCN-induced hepatomegaly can be abolished in *Pxr*-knockout mice [16]. PXR was also found to augment the hepatocyte proliferation induced by the activation of CAR and PPARα [14]. Most recently, we found that PXR could regulate liver size and liver cell fate in a yes-associated protein (YAP)-dependent manner, and PXR-induced

[1]Guangdong Provincial Key Laboratory of New Drug Design and Evaluation, School of Pharmaceutical Sciences, Sun Yat-sen University, Guangzhou 510006, China; [2]Kunming Institute of Botany, Chinese Academy of Sciences, Kunming 650201, China and [3]School of Pharmacy, Southern Medical University, Guangzhou 510515, China
Correspondence: Hui-chang Bi (bihchang@mail.sysu.edu.cn)
These authors contributed equally: Xin-peng Yao, Ting-ying Jiao

Received: 29 December 2020 Accepted: 25 February 2021
Published online: 29 March 2021

hepatomegaly is accompanied with hepatocyte enlargement, proliferation, and induction of a regenerative hybrid hepatocyte reprogramming [17]. As a core factor of Hippo pathway, YAP plays an important role in the control of organ size by directly regulating the downstream genes that are related to cell proliferation and apoptosis [18]. Overexpression of YAP has been reported to contribute to liver enlargement [19].

As mentioned above, Mif can activate PXR, we therefore hypothesized that Mif-induced hepatomegaly is PXR-dependent. This hypothesis was tested using WT and *Pxr*-knockout mice. The interaction between PXR and YAP and their contributions to Mif-induced hepatomegaly were also explored. The current study aimed to study the effect of Mif on liver size during the treatment dose of the CS and pregnancy termination, to investigate the role of PXR and YAP in Mif-induced hepatomegaly, and further verify whether this hepatomegaly is PXR-dependent.

MATERIALS AND METHODS

Chemicals and reagents

Mif with 98% purity (Cat# M126999) and corn oil (Cat# C116025) were purchased from Aladdin Company (Shanghai, China). Rifampicin (RIF) with 97% purity (Cat# R3501) was acquired from Sigma Aldrich (St. Louis, MO, USA). Rabbit polyclonal anti-PXR (Cat# ab192579) was obtained from Abcam Company (Shanghai, China). Rabbit monoclonal anti-PCNA (Cat# 13110S), anti-CTNNB1 (Cat# 8480S), anti-YAP (Cat# 14074S), and anti-β-ACTIN (Cat# 4970S) antibodies were all obtained from Cell Signaling Technology (MA, USA). Mouse monoclonal anti-CYP3A11 (Cat# sc-53850) antibody was purchased from Santa Cruz Biotechnology (Santa Cruz, CA, USA). Rabbit polyclonal anti-CYP2B10 (Cat# A1463) antibody and rabbit polyclonal anti-UGT1A1 (Cat# A6186) antibody were purchased from ABclonal Technology (Wuhan, China). Rabbit polyclonal anti-phosphorylated YAP (Cat# D151452), anti-ANKRD1 (Cat# D121628), anti-CYR61 (Cat# D122190), anti-CTGF (Cat# D160212), and anti-LMNB1 (Cat# D220926) antibodies were acquired from Sangon Biotechnology (Shanghai, China). The pSG5-hPXR expression plasmid was offered by Dr. Steven Kliewer (University of Texas Southwestern Medical Center, Dallas, TX, USA). The pGL3-CYP3A4-XREM-Luc was offered by Dr. Jeff Staudinger (University of Kansas, Lawrence, KS, USA). The pGL4.54-TK control vector plasmid was purchased from Promega (Madison, WI, USA). All the chemical and solvents were commercially available and of analytical or chromatographic grade.

Animal treatments

C57BL/6J male mice (8–10 weeks old) around 20–25 g were purchased from Guangdong Medical Laboratory Animal Center (Guangzhou, China). These mice were housed in a specific pathogen-free room in the laboratory of Animal Center of Sun Yat-sen University. Mice were housed in M2 cages with free access to water and food ad libitum. *Pxr*-knockout mice were kindly provided by Dr. Frank J. Gonzalez at NIH/NCI. Mice were treated with corn oil (0.1 mL/10 g, *i.p.*) or Mif (100 $mg \cdot kg^{-1} \cdot d^{-1}$ or 5 $mg \cdot kg^{-1} \cdot d^{-1}$, *i.p.*) for 5 days. Twenty-four hours after the last injection, mice were sacrificed. The liver and serum samples were collected and stored at −80 °C for further analysis.

All animal treatments and experimental operations were approved by the Institutional Animal Care and Use Committee at Sun Yat-sen University, Guangzhou, China. The whole study strictly complied with the 3Rs principle and ARRIVE guidelines with respect and strictly followed the National Institutes of Health guide for the care and use of Laboratory animals (NIH Publications No. 8023, revised 1978).

Serum biochemical analysis

Serum alkaline phosphatase (ALP), aspartate transaminase (AST), alanine aminotransferase (ALT), total bile acid (TBA), triglyceride (TG) and total cholesterol (T-CHO) levels were measured by the commercially available kits from Nanjing Jiancheng Bioengineering Institute (Nanjing, China) according to the manufacturer's protocols.

Histological analysis

For hematoxylin and eosin (H&E) staining, mice liver tissues were fixed in formalin, embedded, and sectioned. Paraffin-embedded sections were stained by H&E. For immunohistochemical (IHC) staining, paraffin-embedded sections were stained with CTNNB1 antibody (CA#562505, BD Biosciences, San Jose, CA, USA) and Ki67 antibody (CA#15580, Abcam Company, Shanghai, China) after heat-induced epitope retrieval in citrate buffer (pH = 6.0), then visualized by DAB from Vector Company (CA#H-2200, CA, USA).

Real-time quantitative polymerase chain reaction analysis

Total RNA from mice liver were isolated by using Trizol reagent (Invitrogen, Grand Island, NY, USA) and quantified by the NanoDrop spectrophotometer (Thermo Scientific, Rockford, IL, USA) as described previously [20]. Purified RNA was reverse-transcribed to complementary DNA using the PrimeScript RT reagent kit (TaKaRa Biotech, Kyoto, Japan). Real-time quantitative polymerase chain reaction analysis was performed in Biosystems 7500 and using SYBR Premix Ex-Taq II Kit (Takara), which is according to the method reported before [21]. The fold changes of mRNA levels were normalized by the mRNA expression of *Actb* and analyzed by ΔΔCt method. All sequences of primers used in these methods are listed in the supporting information (Supplementary Table 1).

Western blot analysis

Western blot analysis was used to evaluate the protein expression. Methods of total protein extractions and Western blot experiment were performed as our previous study [20, 21]. Briefly, mice liver proteins were extracted using RIPA lysis buffer (Biocolors, Shanghai, China) or nuclear/cytosol extract kit (Nanjing Jiancheng Bioengineering Institute, Nanjing, China). The protein concentration was determined by BCA protein concentration assay kit (Thermo Scientific, Rockford, IL, USA). The proteins were separated in 10% SDS-PAGE gel and electrophoretically transferred onto polyvinylidene fluoride membranes. Blots were blocked with bovine serum albumin or non-fat milk. Membranes were incubated overnight with primary antibodies, and then washed by Tris-buffer. A secondary horseradish peroxidase-conjugated anti-rabbit or anti-mouse IgG antibody was subsequently applied and then washed by Tris-buffer. Then specific bands were visualized using a chemiluminescence detection kit (Engreen Biosystem, Beijing, China).

Dual-luciferase reporter gene assays

Dual-luciferase reporter gene assays were performed according to a previous method [20, 21]. Briefly, HEK293T cells were seeded in 96-well plates without antibiotics. Then, 100 ng pGL3-CYP3A4-XREM-Luc, 50 ng pSG5-hPXR, and 3 ng pGL4.54-TK were transfected into each well by Megatran 1.0 (OriGene, MD, USA). Then the transfection mixtures were replaced with phenol red-free Dulbecco' modified Eagle's medium containing 10% charcoal-stripped delipidated fetal bovine serum (FBS). Transfected cells were treated with Mif (0.625, 2.5, 10 μM) or 10 μM RIF (the positive hPXR agonist). The luciferase activity was measured by a luminometer (Berthold Technologies, Germany) using the Promega Dual-Luciferase Reporter Assay System and following the producer's protocols. Renilla activity was measured to normalize firefly luciferase activity for each well.

HepG2 culture and immunofluorescence double staining

The immunofluorescence double staining assays were performed as described in a previous report [17]. HepG2 cells brought from

ATCC company were cultured in DMEM cultural medium containing 10% FBS. Cells were treated with DMSO (the control group) or 20 μM Mif (the Mif group) for 6 h. Then cells were fixed in 4% paraformaldehyde for 30 min and washed by PBS. After washing, HepG2 cells were incubated with 0.5% Triton X-100 (diluted by PBS) for 10 min at 24 °C. Then, HepG2 cells were incubated with rabbit polyclonal anti-PXR (Santa Cruz, CA, USA) and mouse monoclonal anti-YAP (R&D Systems, MN, USA) overnight at 4 °C. Cells were stained with secondary antibodies including anti-mouse IgG Alexa Fluor 488 and anti-rabbit IgG Alexa Fluor 647 (Cell Signaling Technology, MA, USA). Images were acquired by using a confocal microscope (Olympus FV3000, Japan).

Statistical analysis

All data are presented as the mean ± standard deviation. Two-tailed Student's *t* tests were used to assess the differences between groups using SPSS 23.0 software (IBM Analytics, NY, USA) and GraphPad Prism 6.0 software (GraphPad Software, CA, USA). Differences with P values < 0.05 were considered significant.

RESULTS

Mif induces liver enlargement

High-dose Mif (200–900 mg/d) is approved for the treatment of the CS [22]. The effect of Mif on liver size at high dose was investigated. After a 5-day treatment of 100 $mg \cdot kg^{-1} \cdot d^{-1}$ Mif (*i.p.*), which was converted from the dose used for the CS, a significant morphological liver enlargement was observed in C57BL/6J mice compared to that of the vehicle-treated group treated with 0.1 mL/10 g corn oil (Fig. 1a, b). In the meanwhile, the liver-to-body-weight ratio of the Mif group was 5.82% ± 0.50%, which was 21.25% higher than that of the vehicle group (4.80% ± 0.63%) (Fig. 1c). In order to evaluate the average size of hepatocytes after Mif treatment, the IHC staining of β-catenin (CTNNB1) was performed. The result showed a marked increase in the hepatocyte size around the central vein (CV) area in the Mif group compared to that of the vehicle group (Fig. 1d, e), whereas no difference in the hepatocyte size around the portal vein (PV) area in both two groups (Supplementary Fig. 1a, b). To examine the liver proliferation response, the expressions of Ki67 and PCNA were evaluated by using IHC staining. A robust increase of $Ki67^+$ (Fig. 1f, g) and $PCNA^+$ (Fig. 1h, i) hepatocytes around the PV area was found in the Mif group, whereas the amount of $Ki67^+$ or $PCNA^+$ hepatocytes showed no difference around the CV area in these two groups (Supplementary Fig. 1c–f). Overall, high-dose Mif induced hepatomegaly with hepatocyte enlargement and proliferation.

Mif-induced hepatomegaly is not associated with inflammation and liver injury

Hepatomegaly may be induced by inflammation or hepatoxicity [23]. First, we measured the serum biochemical indexes to find out whether the Mif-induced hepatomegaly was related to liver injury. Serum ALT, AST, and ALP levels of the Mif group and vehicle group were in a normal range (Fig. 2a). There was no significant difference in the levels of serum TBA, T-CHO, and TG between the two groups (Fig. 2a). Furthermore, no liver injury was observed in the H&E staining sections of the Mif group and vehicle group (Fig. 2b). Besides, the mRNA expressions of several inflammation factors including *IL-6*, *IL-10*, *IL-1β*, and *TNF-α* in the liver tissues were measured. Consistent with the biochemical analysis, there was no difference in the mRNA levels of these inflammation factors between the two groups (Fig. 2c). Overall, these data indicated that hepatomegaly induced by Mif (100 mg/kg) was an adaptive or non-adverse reaction that was not related to inflammation and liver injury.

Mif at low dose cannot induce hepatomegaly

Low-dose Mif (25 mg/d) treatment is used for early pregnancy termination and medical abortion in clinical practice [24]. To investigate whether this dose could affect liver size in mice, a low dose of Mif (5 $mg \cdot kg^{-1} \cdot d^{-1}$, which was converted from the dose used for early pregnancy termination) was *i.p.* injected to C57BL/6J mice for 5 days (Fig. 3a). There was no change of liver-to-body-weight ratio and morphology in either the Mif group or vehicle group (Fig. 3b, c). In the meantime, no significant increase in hepatocyte size was observed by CTNNB1 staining, indicating that there was no hepatocyte enlargement induced by low-dose Mif treatment (Fig. 3d, e and Supplementary Fig. 2a, b). Neither PCNA nor Ki67 staining showed difference between the Mif and vehicle group, suggesting that no hepatocyte proliferation was induced by low-dose Mif (Fig. 3f–i). The results of serum biochemical indexes and H&E staining indicated no liver injury in either the Mif or vehicle group (Supplementary Fig. 2c, d). To sum up, low-dose Mif cannot induce hepatomegaly in mice.

Mif is a PXR agonist

Hepatomegaly is known to be associated with PXR activation [15]. Mif was reported to activate PXR in vitro [6]. We further confirmed whether Mif is a hPXR or mPXR agonist. The hepatic mRNA levels of PXR and its downstream genes, including *Cyp3a11*, *Cyp2b10*, and *Ugt1a1*, which are classic phase I or II metabolizing enzymes, were significantly upregulated after 100 mg/kg Mif treatment compared to the vehicle group (Fig. 4a, b). In the meanwhile, the protein levels of CYP3A11, CYP2B10, and UGT1A1 were also significantly upregulated in the Mif group (Fig. 4c, d), indicating that 100 mg/kg Mif treatment activated mPXR in vivo. Besides, the protein level of PXR was significantly upregulated in the Mif group but no significant change in the low-dose Mif group (Supplementary Fig. 3a–d). In addition, to further investigate whether Mif could activate hPXR in vitro, a dual-luciferase reporter gene assay was performed to evaluate the transactivation activity of Mif on PXR in HEK293T cells. The positive control RIF, which is a classic hPXR agonist, significantly enhanced the luciferase activity of the hPXR reporter gene to 2.89 folds compared with the control (Fig. 4e). The luciferase activity was significantly increased to 1.58 and 2.31 folds by Mif at the concentration of 2.5 and 10 μM, respectively, whereas remained unchanged at 0.625 μM (Fig. 4e). These results suggested that Mif could induce hPXR in a concentration-dependent manner, and low concentration of Mif cannot activate hPXR. Taken together, these results revealed that Mif could modulate mPXR and its target proteins, and activate hPXR.

Mif induces hepatomegaly with the involvement of PXR/YAP activation

According to our previous research, hepatomegaly induced by PXR activation is related to YAP [17]. We further identified whether Mif could induce YAP activation. The protein levels of total and nuclear YAP in the Mif group were significantly higher than the vehicle group, while the expression of phosphorylated-YAP in cytoplasm was lower (Fig. 5a, b). Furthermore, the expressions of YAP-downstream proteins including connective tissue growth factor (CTGF) and ankyrin repeat domain protein (ANKRD) in the Mif group were markedly upregulated, whereas the protein level of cysteine-rich angiogenic inducer 61 (CYR61) was unchanged (Fig. 5c, d). These results indicated that YAP was activated by Mif. A PXR/YAP immunofluorescence double staining experiment was performed in HepG2 cells to further determine whether PXR and YAP translocated to nucleus together after Mif treatment. No nuclear translocation was observed in the vehicle group (Fig. 5e). But after Mif treatment at 20 μM, a translocation of YAP and PXR to the nucleus was observed. The merge channel showed that the fluorescence of both YAP and PXR was overlapped in the nucleus, suggesting the nuclear translocation of both PXR and YAP (Fig. 5e).

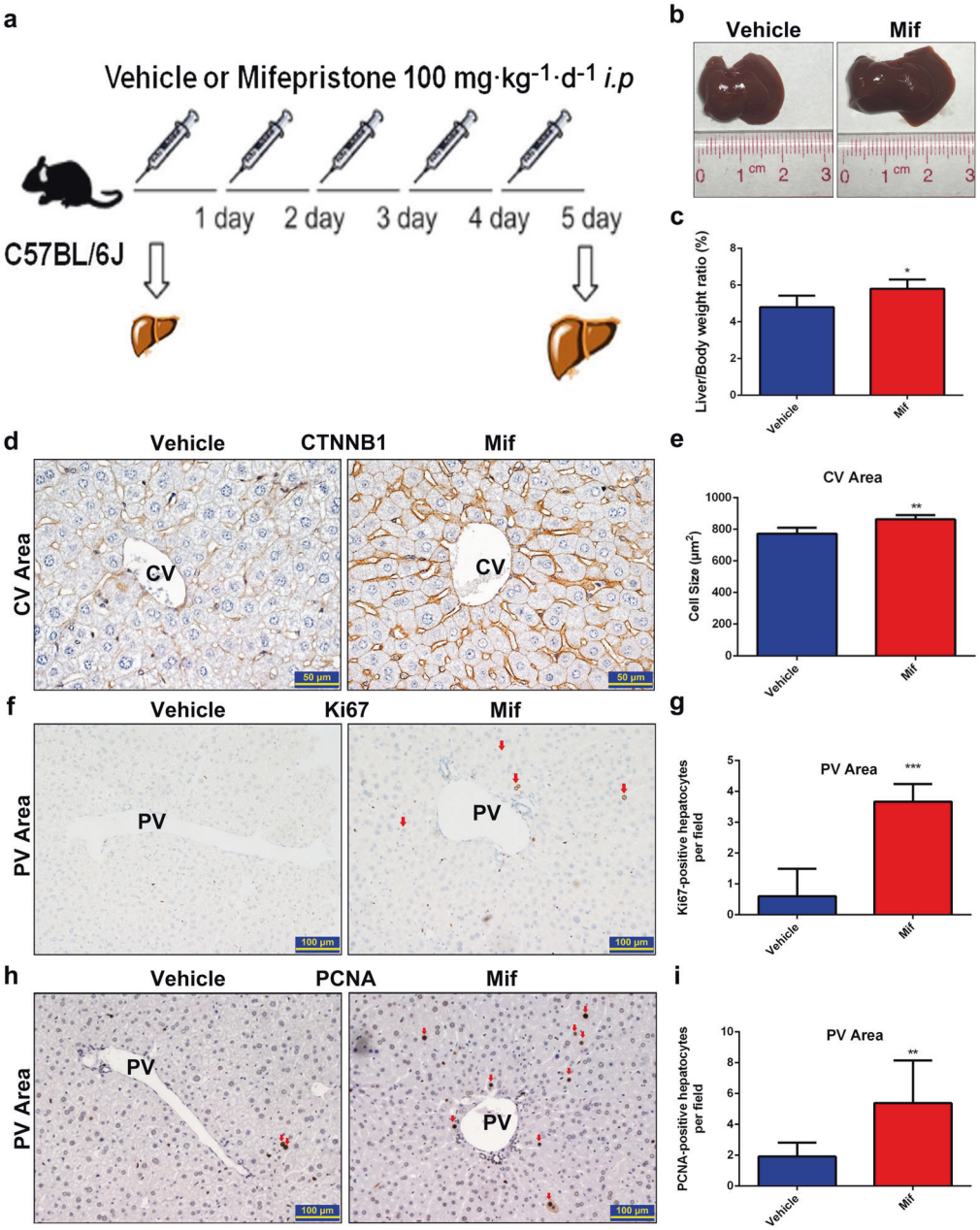

Fig. 1 Mif at 100 mg/kg induces liver enlargement. **a** C57BL/6 mice were treated with the vehicle (corn oil, 0.1 mL/10 g, *i.p.*) or Mif (100 mg · kg^{-1} · d^{-1}, *i.p.*) for 5 days. **b** Representative morphological liver pictures of the vehicle and Mif group. **c** Liver-to-body-weight ratios of the vehicle and Mif group. **d** IHC staining of CTNNB1 measuring hepatocyte size around the CV area of the vehicle- or Mif-treated mice. **e** Quantification of the hepatocyte size around the CV area. **f** IHC staining of Ki67 of liver sections around the PV area of the vehicle- or Mif-treated mice. **g** Quantification of Ki67$^+$ hepatocytes around the PV area. **h** IHC staining of PCNA of liver sections around the PV area of the vehicle- or Mif-treated mice. **i** Quantification of PCNA$^+$ hepatocytes around the PV area. The data are shown as mean ± S.D. ($n = 5$–6) and $^*P < 0.05$, $^{**}P < 0.01$ versus the vehicle group.

These results revealed that Mif treatment could induce nuclear translocation of PXR and YAP, activate YAP, and potentially induce PXR/YAP interaction. To sum up, these data indicated that Mif induces hepatomegaly possibly by PXR/YAP activation.

Mif-induced hepatomegaly is PXR dependent

To further investigate whether Mif-induced hepatomegaly is dependent on PXR activation, *Pxr*-knockout mice were used in this study. The cycle threshold (C_T) values of *Actb* and *Pxr* showed that *Pxr* were knock out efficiently in both the KO-vehicle group and KO-Mif group (Supplementary Fig. 4a). After treated with 100 mg · kg^{-1} · d^{-1} Mif (*i.p.*) or 0.1 mL/10 g/d corn oil (*i.p.*) for 5 days (Fig. 6a), no change in liver size and liver-to-body-weight ratios was observed in the Mif-treated *Pxr*-knockout mice (KO-Mif) compared with the vehicle-treated *Pxr*-knockout mice (KO-vehicle) (Fig. 6b, c). The IHC staining of CTNNB1 showed no significant difference in the hepatocyte size between the KO-Mif and KO-vehicle group (Fig. 6d). Furthermore, there were no detectable Ki67$^+$ or PCNA$^+$ hepatocytes in liver slices of the KO-Mif and KO-vehicle group, suggesting that Mif cannot promote hepatocyte proliferation in *Pxr*-knockout mice (Fig. 6e, f). No liver injury and hepatoxicity was found in two groups as indicated by H&E staining and serum biochemical analysis (Supplementary Fig. 4b, c). There was no significant difference in the protein levels of

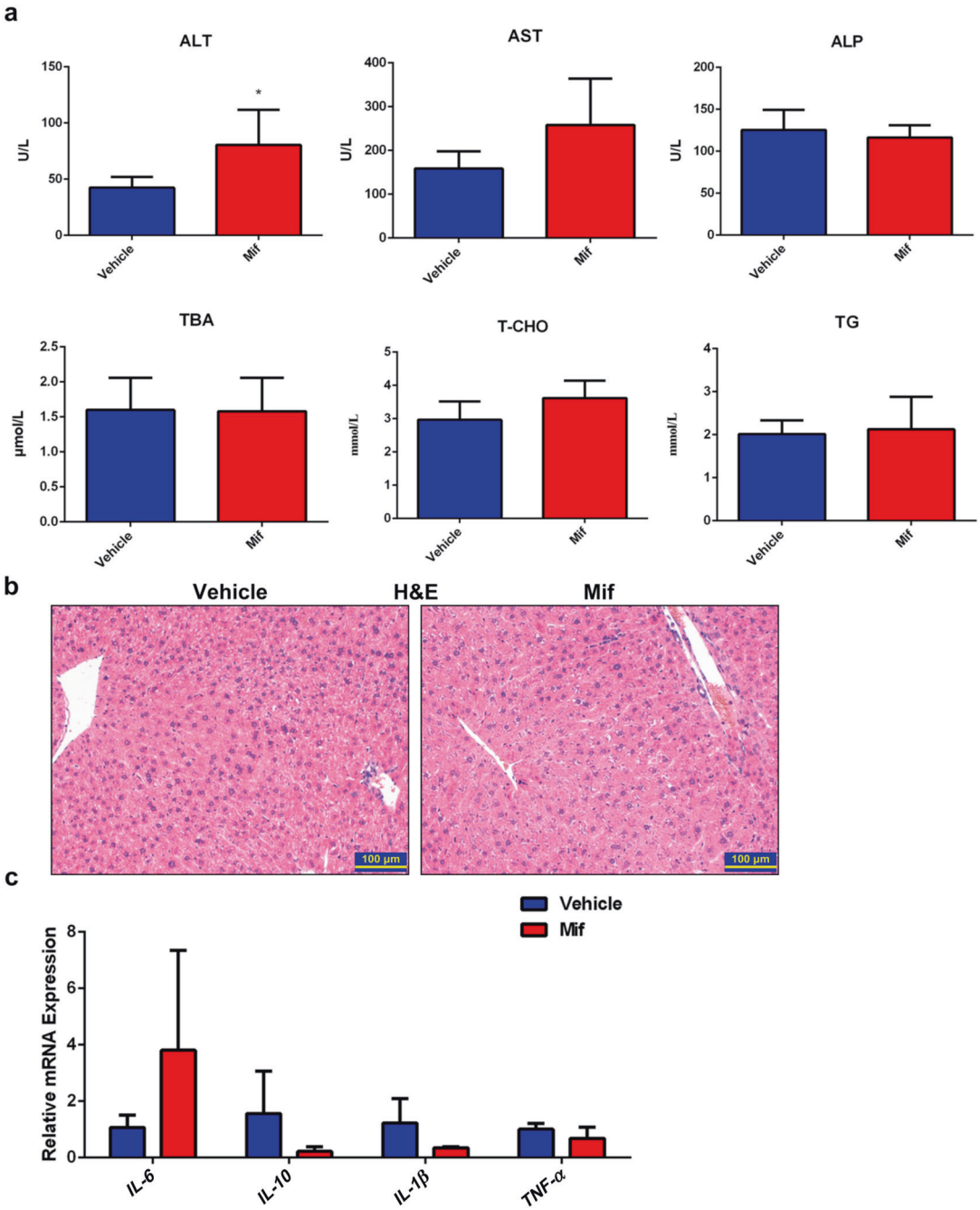

Fig. 2 Mif-induced hepatomegaly is not associated with inflammation and liver injury. a Serum biochemical indexes including ALT, AST, ALP, TBA, T-CHO and TG of the vehicle or Mif group. **b** Representative H&E staining of liver slices of the vehicle or Mif group. **c** The hepatic mRNA expression of *IL-6, IL-10, IL-1β*, and *TNF-α* in livers of the vehicle- or Mif-treated mice. The data are presented as means ± S.D. ($n = 5–6$) and $^{*}P < 0.05$ versus the vehicle group.

CYP2B10, CYP3A11, and UGT1A1 between two groups, suggesting that PXR pathway was not activated after Mif treatment in *Pxr*-knockout mice (Fig. 6g, h). Overall, these results demonstrated that Mif induced hepatomegaly in a PXR-dependent way.

DISCUSSION

It has been reported that high dose of Mif could induce hepatomegaly in mice and rats. However, the pathophysiological characteristics and the related mechanism of the Mif-induced hepatomegaly remain unknown. In this study, we first confirmed that high-dose Mif (100 mg/kg) could induce benign hepatomegaly in mice, which was accompanied with hepatocyte enlargement and proliferation. Furthermore, Mif induced nuclear translocation of PXR and YAP, and activation of PXR and YAP, indicating the involvement of PXR and YAP in Mif-induced hepatomegaly. Finally, *Pxr*-knockout mice were used to confirm that Mif-induced hepatomegaly was PXR-dependent. Therefore, this study revealed that PXR can mediate Mif-induced hepatomegaly by interaction with YAP pathway.

Different doses of Mif are used for the treatment of different diseases. The daily dose range of Mif for the treatment of CS is 200–900 mg/d, and this range of dose could be converted into 44–185 $mg \cdot kg^{-1} \cdot d^{-1}$ in mice [22]. Mif treatment at 50–150 mg/d

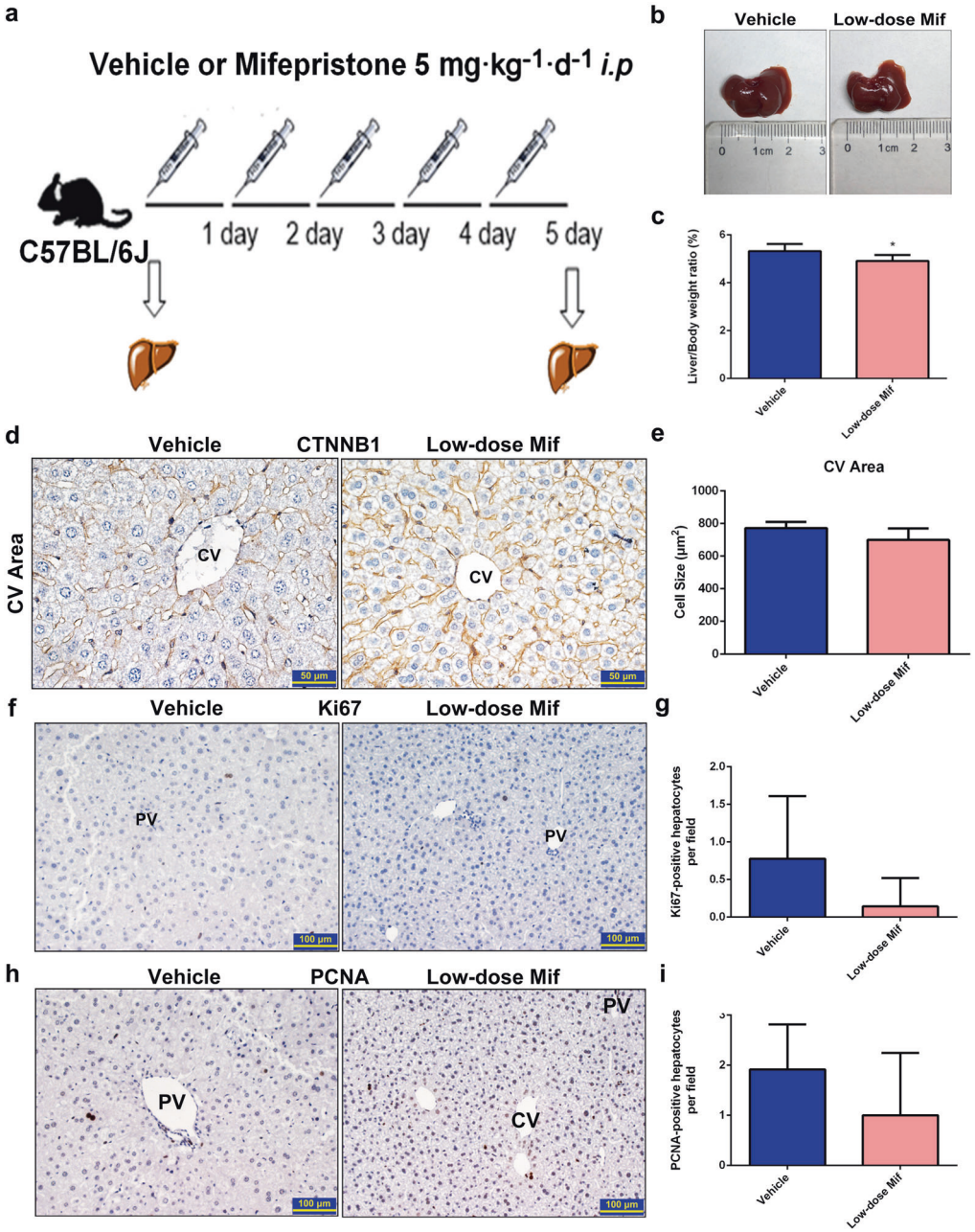

Fig. 3 **Low-dose Mif cannot induce hepatomegaly. a** C57BL/6 mice were treated with the vehicle (corn oil, 0.1 mL/10 g, *i.p.*) or low-dose Mif (Mif, 5 mg · kg^{-1} · d^{-1}, *i.p.*) for 5 days. **b** Representative morphological liver pictures of the vehicle or Mif group. **c** Liver-to-body-weight ratios of the vehicle or Mif group. **d** IHC staining of CTNNB1 measuring hepatocyte size around the CV area of the vehicle and Mif group. **e** Quantification of the hepatocytes size around the CV area. **f** IHC staining of Ki67 of liver sections of the vehicle and Mif group. **g** Quantification of Ki67^{+} hepatocytes **h** IHC staining of PCNA of liver sections of the vehicle and Mif group. **i** Quantification of PCNA^{+} hepatocytes. The data are shown as mean ± S.D. ($n = 5$–6) and $^{*}P < 0.05$ versus the vehicle group.

or even 25 mg/d for 2 days is usually used for the very early pregnancy termination. And 50 mg/d Mif for 3 months could be used for uterine leiomyomata [24–26]. The range of dose above could be converted into 5–30 mg · kg^{-1} · d^{-1} in mice. In the current study, doses of 100 and 5 mg · kg^{-1} · d^{-1} were used to study the effect of different doses of Mif on the liver size in mice. Since endometrium is the most sensitive target-organ to Mif [27, 28], male mice were used to investigate the effect of Mif on liver size. In this study, Mif at 100 mg · kg^{-1} · d^{-1} was confirmed to induce hepatomegaly in mice, whereas 5 mg · kg^{-1} · d^{-1} Mif had no effect on the size of mice liver.

Liver inflammation and injury are often considered as the causes of hepatomegaly [9, 23]. It is essential to distinguish non-adverse (adaptive) from adverse hepatomegaly [9]. According to the guidance from Health and Safety Executive (UK), two steps must be carefully considered to conclude whether this hepatomegaly is adverse or not [10]. The first step is to assess the histological evidence of structural degenerative or necrotic changes, and the second one is to assess clinical pathology evidence of some biochemical indexes associated with hepatocyte damage [10]. In the current study, hepatomegaly induced by Mif was not accompanied with liver injury as evidenced by the H&E

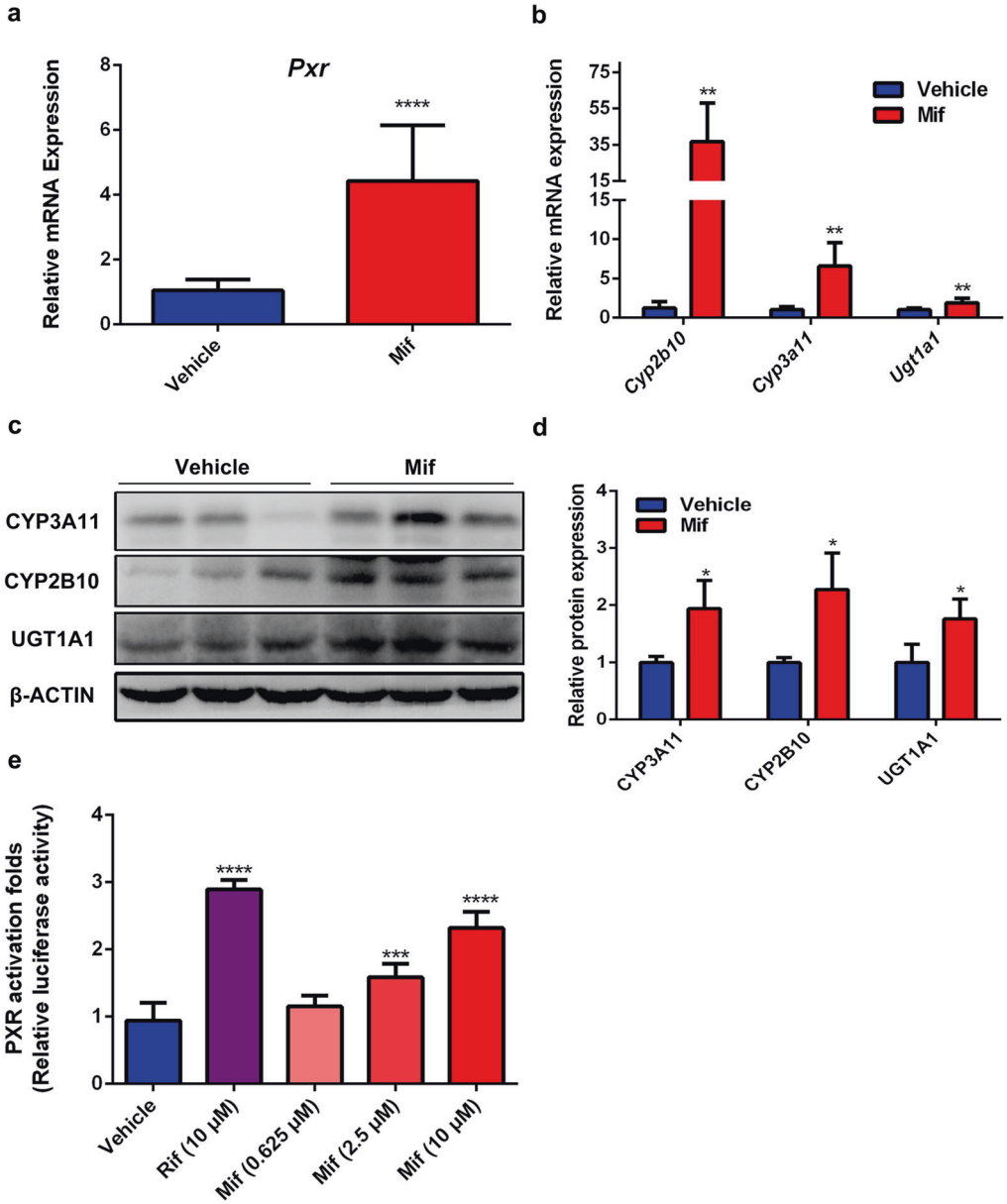

Fig. 4 Mif is a PXR agonist. a The hepatic *Pxr* mRNA levels of the vehicle or Mif group. **b** The hepatic *Cyp3a11*, *Cyp2b10* and *Ugt1a1* mRNA levels of the vehicle or Mif group. **c** The hepatic protein expression levels of PXR downstream targets of the vehicle or Mif group. **d** Quantification of CYP3A11, CYP2B10 and UGT1A1 protein levels normalized to the expression of β-ACTIN. **e** Dual-luciferase reporter gene assay was used to determine the effect of RIF or different concentrations of Mif on hPXR activation in HEK293T cells. The data are expressed as mean ± S.D. $^{*}P < 0.05$, $^{**}P < 0.01$, $^{***}P < 0.001$ and $^{****}P < 0.0001$ compared with the vehicle group ($n = 3–5$).

staining and biochemical analysis. Moreover, the mRNA levels of inflammation factors also showed no significant change. PXR plays an important role in inflammation response. For example, nuclear factor-κB signaling, a key factor involving the process of the innate and adaptive immune responses, is significantly inhibited following PXR activation, which thereby reduces the expression of its target genes including *TNFα*, *IL-10*, and *IL-1β* [29–32]. And lipopolysaccharide-induced inflammatory response in liver can be reduced by induction of cytochrome P450 metabolizing enzymes regulated by PXR [33]. This implicates an inhibitory effect of PXR on inflammation response. Besides, there is no reasonable evidence that the inhibition of inflammation response is associated with hepatomegaly. Thus, PXR-induced hepatomegaly is not associated with inflammation, which is consistent with our results that no significant change but a declining trend in the mRNA levels of inflammatory factors *TNFα*, *IL-10*, and *IL-1β*, and no observed infiltration of immunocytes, vasodilation, and hepatocyte edema in the H&E staining in Mif-induced hepatomegaly are found. Thus, Mif-induced hepatomegaly is not associated with inflammation and liver injury and could be considered as a benign (non-adverse) hepatomegaly.

Hepatocyte proliferation is considered as one of the major causes of hepatomegaly. For example, CAR activation could induce liver enlargement accompanied with hepatocyte proliferation without liver injury, and this effect could be augmented by PXR activation [14, 34]. Ki67 and PCNA are two biomarkers of hepatocyte proliferation [35, 36]. The expressions of Ki67 and PCNA have regional difference between the CV and PV areas. This finding is consistent with our previous study [17]. As blood floods from the PV area to CV area, the hemodynamic differences between these two areas result in differences of oxygen supplement and nutritional status [37]. Hepatocyte proliferation

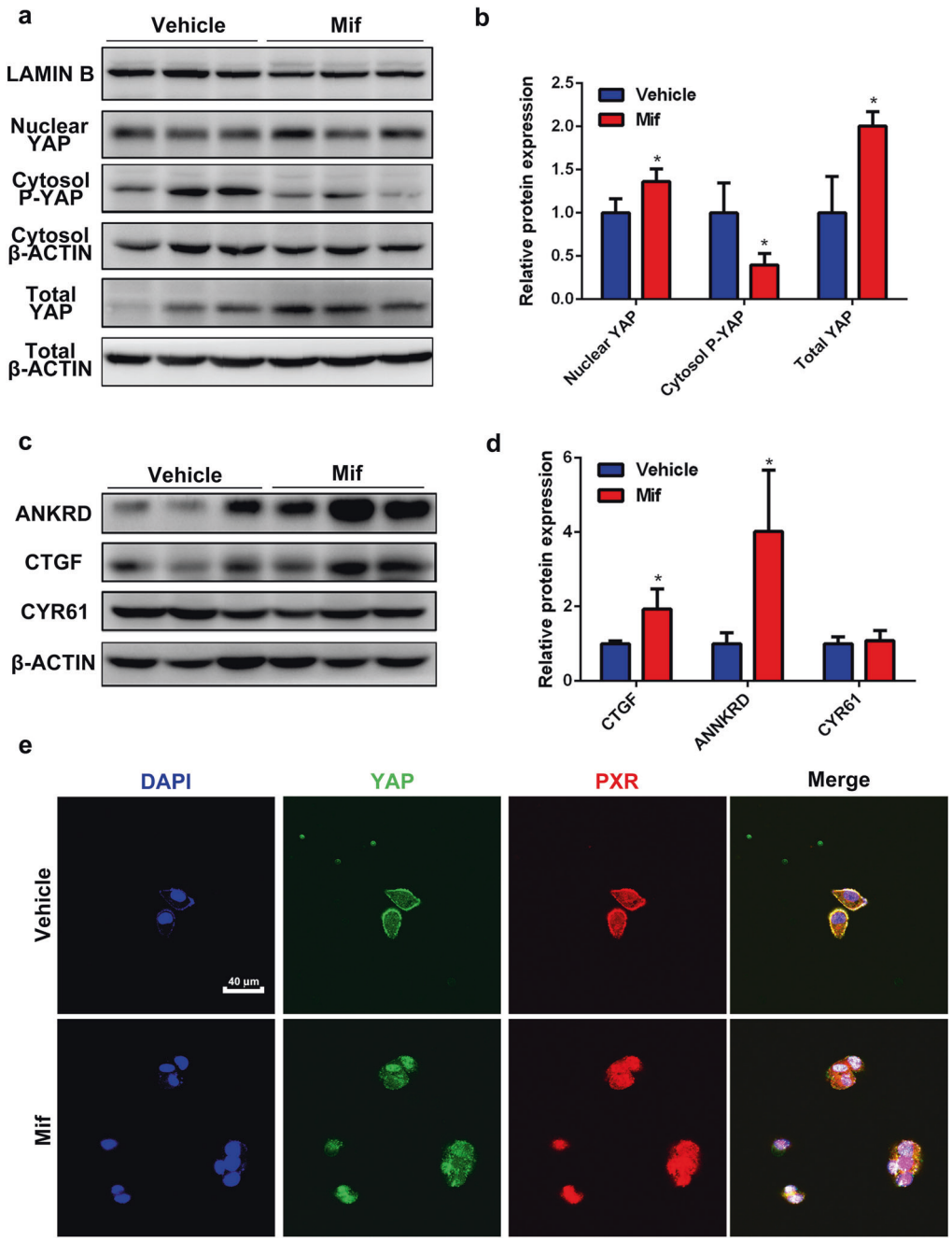

Fig. 5 Mif-induced hepatomegaly is associated with the PXR/YAP activation. **a** The hepatic protein levels of nuclear YAP, total YAP and cytosol-p-YAP of the vehicle or Mif group. **b** Quantification of total YAP, cytoplasmic p-YAP and nuclear YAP normalized to the expression of β-ACTIN. **c** The hepatic protein levels of YAP downstream targets including ANKRD, CTGF and CYR61 of the vehicle or Mif group. **d** Quantification of ANKRD, CTGF and CYR61 normalized to the expression of β-ACTIN. **e** Immunofluorescence double-staining experiment of PXR and YAP in HepG2 cells. The data are expressed as the mean ± S.D. $^*P < 0.05$ compared with the vehicle group ($n = 3$).

is mainly located around the PV area where the concentrations of oxygen and nutrition are high. In the current study, 100 mg/kg Mif was found to induce hepatomegaly accompanied by hepatocyte proliferation mainly around PV area, implicating that hepatocyte proliferation contributed to the Mif-induced hepatomegaly.

Interestingly, Mif-induced hepatomegaly was found to be accompanied by hepatocyte enlargement around the CV area but not the PV area in the liver. Bile formation, glucose synthesis, and cholesterol synthesis are mainly located around the PV area; glycolysis, lipogenesis, and xenobiotic metabolism are mainly located around the CV area [37]. According to a recent study, about 50% genes in the liver are significantly zonated among the liver lobules and the drug metabolizing enzymes such as cytochrome-P450s are mainly located in the CV area [38]. It has been reported that the induction of metabolizing enzymes by NRs is one of the main causes of hepatomegaly [9], which indicated that hepatocyte enlargement induced by Mif around CV area may be related to the increased metabolizing enzymes induced by NRs especially by PXR.

PXR plays a critical role in the endobiotics homeostasis, xenobiotics disposition, and energy metabolism in vivo. In the current study, mPXR activation was confirmed by upregulated CYP3A11, CYP2B10, and UGT1A1 in both mRNA and protein levels. Although mPXR and hPXR have nearly 95% homology in their

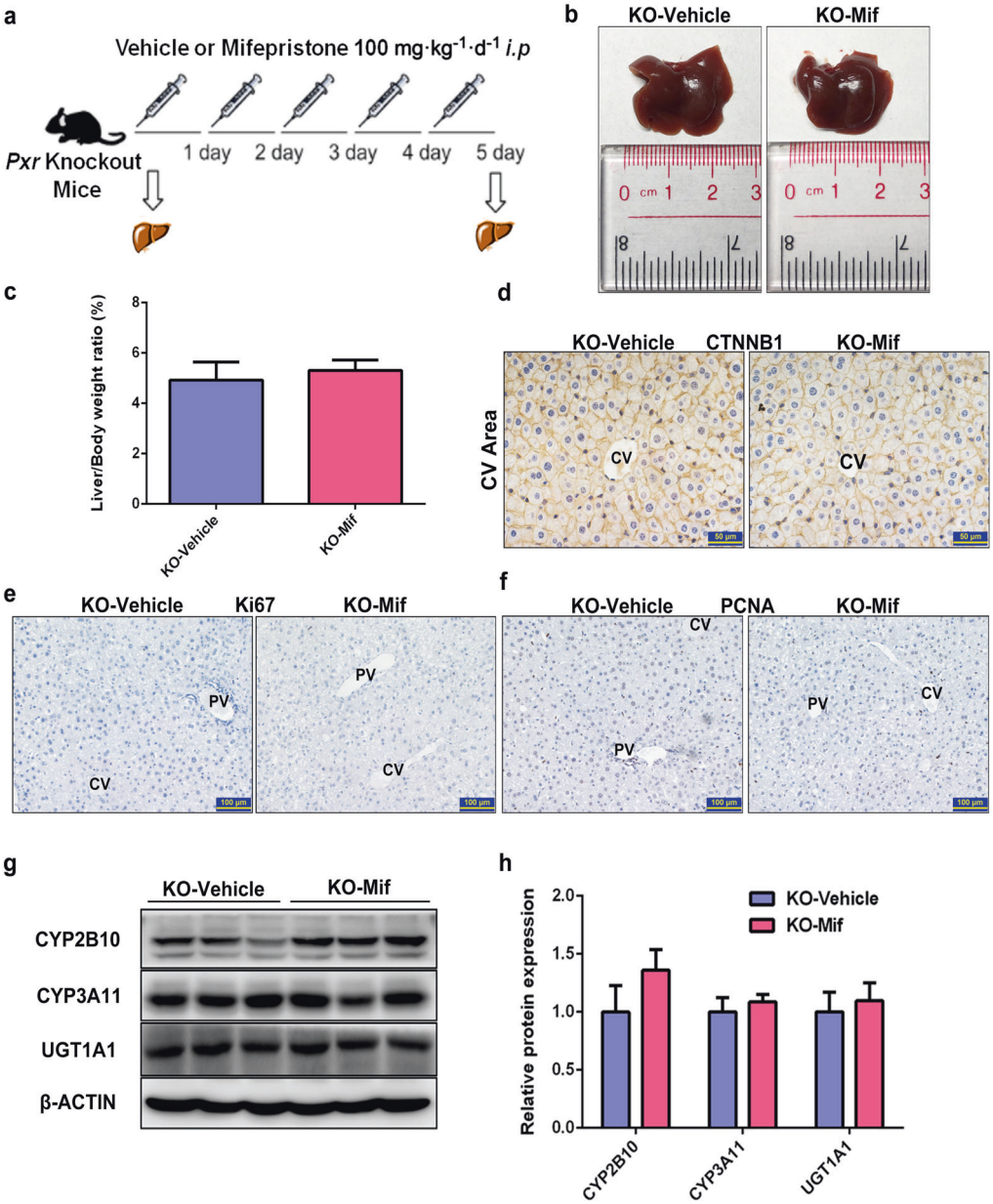

Fig. 6 Mif-induced hepatomegaly is PXR-dependent. a *Pxr*-knockout mice were treated with the vehicle (corn oil, 0.1 mL/10 g, *i.p.*) or Mif (100 mg · kg^{-1} · d^{-1}, *i.p.*) for 5 days. **b** Representative morphological liver pictures of the KO-vehicle and KO-Mif group. **c** Liver-to-body-weight ratios of the KO-vehicle and KO-Mif group. **d** IHC staining of CTNNB1 measuring hepatocyte size around the CV area of the KO-vehicle and KO-Mif group. **e** IHC staining of Ki67 of mice liver of the KO-vehicle and KO-Mif group. **f** IHC staining of PCNA of mice liver of the KO-vehicle and KO-Mif group. **g** The hepatic protein levels of PXR downstream targets such as CYP2B10, CYP3A11 and UGT1A1 of *Pxr*-knockout mice treated with the vehicle or Mif. **h** Quantification of CYP2B10, CYP3A11 and UGT1A1 normalized to the expression of β-ACTIN. The data are shown as mean ± S.D. ($n = 3$–6).

DNA-binding domain, they only have 73% homology in ligand-binding domain [39]. It has been proved that Mif could activate both mPXR and hPXR in vitro [6]. Moreover, the mRNA and protein levels of PXR were both upregulated by high-dose Mif according to our study that indicated that Mif upregulates PXR expression in the liver and the increased expressions of PXR downstream proteins in the Mif group are not only due to PXR activation but also potentially due to the increased expression of PXR. This is consistent with a previous finding that Mif can not only act as a PXR activator, but also induce the mRNA expression of PXR in vivo and in vitro [40]. At doses of Mif in 22.5, 45, and 90 mg/kg (*p.o.*) in male rats, which can be converted to 32.5, 65.52, and 131.04 mg/kg in mice based on equivalent body surface area, the plasma concentrations of Mif (C_{max}) were 0.15, 0.46, and 0.96 μg/mL according to a pharmacokinetic study [41]. Here, we evaluated the hPXR activity of Mif at concentrations of 0.625, 2.5, and 10 μM (0.27, 1.07, and 4.30 μg/mL in mice). The concentration of 2.5 μM is approximately equivalent to the plasma concentration of mice after the administration of 131.04 mg/kg of Mif, which is close to the dose of Mif (100 mg/kg) in our study. According to results of dual-luciferase reporter gene assays, 2.5 μM of Mif could significantly activate hPXR, which is consistent with the result that high-dose Mif (100 mg/kg) can activate PXR pathway and induce hepatomegaly in mice. In addition, 0.625 μM Mif cannot activate hPXR, which is consistent with the result that low-dose Mif (5 mg/kg) cannot induce hepatomegaly in mice. Therefore,

high-dose Mif was confirmed to induce PXR activation in a dose-dependent manner both in vivo and in vitro. Thus, hepatomegaly induced by high-dose Mif (100 mg/kg) could be related to PXR activation.

YAP, which is a critical factor of Hippo pathway, plays an important role in the regulation of organ size by directly regulating the proliferation-related genes [18]. Phosphorylation of YAP increases its cytoplasmic retention and inhibits its function as a transcriptional co-activator in the nucleus [42]. YAP overexpression enlarged the liver and promoted hepatocyte proliferation [19]. We previously reported that PXR activation can induce liver enlargement via YAP signaling pathway [17]. In this study, YAP pathway has been activated after Mif treatment as demonstrated by upregulation of total and nuclear YAP, as well as the downstream proteins of YAP such as CTGF and ANKRD. Besides, both PXR and YAP are commonly located in the cytoplasm and they could translocate into the nucleus after activation [43, 44]. Here, nuclear translocation of both PXR and YAP was also observed in HepG2 cells after Mif treatment, indicating a possible interaction of PXR and YAP as previously reported [17]. These results indicated that Mif could induce YAP activation and probably induce PXR and YAP interaction.

Since Mif-induced hepatomegaly is highly similar to the PXR-induced hepatomegaly, which is accompanied with hepatocyte enlargement and proliferation without liver injury and inflammation [23], it is reasonable to assume that PXR plays a crucial role in Mif-induced hepatomegaly. *Pxr*-knockout mice were used to further confirm whether such a hepatomegaly is PXR dependent. The results demonstrated that Mif-induced hepatomegaly was abolished in *Pxr*-knockout mice, and the cell size and proliferation of hepatocytes were also unaffected as evidenced by CTNNB1, PCNA, and Ki67 staining. These findings indicated that Mif-induced liver enlargement depends on PXR pathway. However, since benign hepatomegaly may develop to an adverse effect at high dose or following prolonged exposure of drugs [45, 46], it is necessary to evaluate whether Mif can induce adverse hepatomegaly in a higher dose or a longer-period treatment. Since Mif is used more frequently in female patients than males, this phenomenon should be further confirmed in female animal models in the future.

Mif could activate both human- and mouse-PXR at high dose according to our study, which indicates that potential drug–drug interaction (DDI) could happen and more attention should be paid for those patients who are taking high-dose Mif for CS. Many DDIs are caused by PXR-mediated transcriptional activation of phase I/II drug metabolizing enzymes or drug transporters [47]. It has been reported that the cytochrome P450 metabolizing enzymes 3A4, 2B6, and 2C9, which are the main metabolizing enzymes, are regulated by PXR [48, 49]. Increased levels of drug metabolizing enzymes may result in a reduction of plasma concentrations of drugs and decrease in efficiency. Furthermore, the elevation of drug metabolites may cause toxicity.

In summary, the current study demonstrated that high-dose Mif used for the treatment of CS can induce hepatomegaly with significant hepatocyte enlargement and proliferation. This hepatomegaly is a benign but not an adverse effect. Furthermore, the hepatomegaly induced by Mif is dependent on PXR activation and possibly due to its interaction with YAP. This study provides new insights in the effect of Mif at different dosages on the liver size and the clinical rational use of Mif, and provides novel evidences on the crucial function of PXR agonist in liver enlargement and regeneration.

ACKNOWLEDGEMENTS

The work was supported by the National Natural Science Foundation of China (Grants: 81973392, 82025034); the National Key Research and Development Program (Grant: 2017YFE0109900); the Shenzhen Science and Technology Program (KQTD20190929174023858); the Natural Science Foundation of Guangdong (Grant: 2017A030311018); the 111 project (Grant: B16047); the Key Laboratory Foundation of Guangdong Province (Grant: 2017B030314030); the Local Innovative and Research Teams Project of Guangdong Pearl River Talents Program (2017BT01Y093); and the National Engineering and Technology Research Center for New drug Druggability Evaluation (Seed Program of Guangdong Province, 2017B090903004).

AUTHOR CONTRIBUTIONS

XPY, TYJ, MH, and HCB participated in research design. XPY, TYJ, SCF, YYZ, YMJ, FL, XY, PPC, and YG performed experiments. XPY, TYJ, and HCB wrote or revised the manuscript.

ADDITIONAL INFORMATION

Supplementary information The online version contains supplementary material available at https://doi.org/10.1038/s41401-021-00633-4.

Competing interests: The authors declare no competing interests.

REFERENCES

1. Ulmann A, Teutsch G, Philibert D. RU 486. Sci Am. 1990;262:42–8.
2. Avrech OM, Golan A, Weinraub Z, Bukovsky I, Caspi E. Mifepristone (RU486) alone or in combination with a prostaglandin analogue for termination of early pregnancy: a review. Fertil Steril. 1991;56:385–93.
3. Chen J, Wang J, Shao J, Gao Y, Xu J, Yu S, et al. The unique pharmacological characteristics of mifepristone (RU486): from terminating pregnancy to preventing cancer metastasis. Med Res Rev. 2014;34:979–1000.
4. Bamberger CM, Chrousos GP. The glucocorticoid receptor and RU 486 in man. Ann N Y Acad Sci. 1995;761:296–310.
5. Nieman LK, Biller BM, Findling JW, Murad MH, Newell-Price J, Savage MO, et al. Treatment of Cushing's syndrome: an Endocrine Society clinical practice guideline. J Clin Endocrinol Metab. 2015;100:2807–31.
6. Vignati LA, Bogni A, Grossi P, Monshouwer M. A human and mouse pregnane X receptor reporter gene assay in combination with cytotoxicity measurements as a tool to evaluate species-specific CYP3A induction. Toxicology. 2004;199:23–33.
7. Xiao Y, Zhu Y, Yu S, Yan C, Ho RJ, Liu J, et al. Thirty-day rat toxicity study reveals reversible liver toxicity of mifepristone (RU486) and metapristone. Toxicol Mech Methods. 2016;26:36–45.
8. Wang J, Chen J, Zhu Y, Zheng N, Liu J, Xiao Y, et al. In vitro and in vivo efficacy and safety evaluation of metapristone and mifepristone as cancer metastatic chemopreventive agents. Biomed Pharmacother. 2016;78:291–300.
9. Hall AP, Elcombe CR, Foster JR, Harada T, Kaufmann W, Knippel A, et al. Liver hypertrophy: a review of adaptive (adverse and non-adverse) changes–conclusions from the 3rd International ESTP Expert Workshop. Toxicol Pathol. 2012;40:971–94.
10. Andrew D. PSD Guidance Document. Interpretation of liver enlargement in regulatory toxicity studies, 2005. https://webarchive.nationalarchives.gov.uk/20121031084609/http://www.pesticides.gov.uk/Resources/CRD/Migrated-Resources/Documents/A/ACP_Paper_on_the_interpretation_of_Liver_Enlargement.pdf.
11. Bookout AL, Jeong Y, Downes M, Yu RT, Evans RM, Mangelsdorf DJ. Anatomical profiling of nuclear receptor expression reveals a hierarchical transcriptional network. Cell. 2006;126:789–99.
12. Huang W, Zhang J, Washington M, Liu J, Parant JM, Lozano G, et al. Xenobiotic stress induces hepatomegaly and liver tumors via the nuclear receptor constitutive androstane receptor. Mol Endocrinol. 2005;19:1646–53.
13. Cattley RC. Regulation of cell proliferation and cell death by peroxisome proliferators. Microsc Res Tech. 2003;61:179–84.
14. Shizu R, Benoki S, Numakura Y, Kodama S, Miyata M, Yamazoe Y, et al. Xenobiotic-induced hepatocyte proliferation associated with constitutive active/androstane receptor (CAR) or peroxisome proliferator-activated receptor α (PPARα) is enhanced by pregnane X receptor (PXR) activation in mice. PLoS ONE. 2013;8:e61802.
15. Garg BD, Kovacs K, Tuchweber B, Khandekar JD. Effect of pregnenolone-16alpha-carbonitrile, a microsomal enzyme inducer, on the regenerating rat liver. Acta Anat (Basel). 1975;91:161–74.
16. Staudinger J, Liu Y, Madan A, Habeebu S, Klaassen CD. Coordinate regulation of xenobiotic and bile acid homeostasis by pregnane X receptor. Drug Metab Dispos. 2001;29:1467–72.
17. Jiang Y, Feng D, Ma X, Fan S, Gao Y, Fu K, et al. Pregnane X receptor regulates liver size and liver cell fate by yes-associated protein activation in mice. Hepatology. 2019;69:343–58.

18. Nguyen Q, Anders RA, Alpini G, Bai H. Yes-associated protein in the liver: Regulation of hepatic development, repair, cell fate determination and tumorigenesis. Dig Liver Dis. 2015;47:826–35.
19. Camargo FD, Gokhale S, Johnnidis JB, Fu D, Bell GW, Jaenisch R, et al. YAP1 increases organ size and expands undifferentiated progenitor cells. Curr Biol. 2007;17:2054–60.
20. Zeng H, Jiang Y, Chen P, Fan X, Li D, Liu A, et al. Schisandrol B protects against cholestatic liver injury through pregnane X receptors. Br J Pharmacol. 2017;174: 672–88.
21. Zeng H, Li D, Qin X, Chen P, Tan H, Zeng X, et al. Hepatoprotective effects of *Schisandra sphenanthera* extract against lithocholic acid-induced cholestasis in male mice are associated with activation of the pregnane X receptor pathway and promotion of liver regeneration. Drug Metab Dispos. 2016;44:337–42.
22. Yuen KC, Williams G, Kushner H, Nguyen D. Association between mifepristone dose, efficacy, and tolerability in patients with Cushing syndrome. Endocr Pract. 2015;21:1087–92.
23. Carthew P, Nolan BM, Edwards RE, Smith LL. The role of cell death and cell proliferation in the promotion of rat liver tumours by tamoxifen. Cancer Lett. 1996;106:163–9.
24. Li CL, Chen DJ, Sheng XJ, Liu MX, Weng HN, Du PL, et al. The lowest dosages of mifepristone and misoprostol to terminate ultra-early pregnancy. Zhonghua Fu Chan Ke Za Zhi. 2012;47:764–8.
25. Song LP, Tang SY, Li CL, Zhou LJ, Mo XT. Early medical abortion with self-administered low-dose mifepristone in combination with misoprostol. J Obstet Gynaecol Res. 2018;44:1705–11.
26. Murphy AA, Kettel LM, Morales AJ, Roberts VJ, Yen SS. Regression of uterine leiomyomata in response to the antiprogesterone RU 486. J Clin Endocrinol Metab. 1993;76:513–7.
27. Gemzell-Danielsson K, Westlund P, Johannisson E, Swahn ML, Bygdeman M, Seppala M. Effect of low weekly doses of mifepristone on ovarian function and endometrial development. Hum Reprod. 1996;11:256–64.
28. Batista MC, Cartledge TP, Zellmer AW, Merino MJ, Axiotis C, Loriaux DL, et al. Delayed endometrial maturation induced by daily administration of the antiprogestin RU 486: a potential new contraceptive strategy. Am J Obstet Gynecol. 1992;167:60–5.
29. Jacobs MD, Harrison SC. Structure of an IkappaBalpha/NF-kappaB complex. Cell. 1998;95:749–58.
30. Gu X, Ke S, Liu D, Sheng T, Thomas PE, Rabson AB, et al. Role of NF-kappaB in regulation of PXR-mediated gene expression: a mechanism for the suppression of cytochrome P-450 3A4 by proinflammatory agents. J Biol Chem. 2006;281: 17882–9.
31. Cheng J, Shah YM, Gonzalez FJ. Pregnane X receptor as a target for treatment of inflammatory bowel disorders. Trends Pharmacol Sci. 2012;33:323–30.
32. Shah YM, Ma X, Morimura K, Kim I, Gonzalez FJ. Pregnane X receptor activation ameliorates DSS-induced inflammatory bowel disease via inhibition of NF-kappaB target gene expression. Am J Physiol Gastrointest Liver Physiol. 2007;292: G1114–22.
33. Moriya N, Kataoka H, Fujino H, Nishikawa J, Kugawa F. Effect of lipopolysaccharide on the xenobiotic-induced expression and activity of hepatic cytochrome P450 in mice. Biol Pharm Bull. 2012;35:473–80.
34. Blanco-Bose WE, Murphy MJ, Ehninger A, Offner S, Dubey C, Huang W, et al. C-Myc and its target FoxM1 are critical downstream effectors of constitutive androstane receptor (CAR) mediated direct liver hyperplasia. Hepatology. 2008;48:1302–11.
35. Gerdes J, Lemke H, Baisch H, Wacker HH, Schwab U, Stein H. Cell cycle analysis of a cell proliferation-associated human nuclear antigen defined by the monoclonal antibody Ki-67. J Immunol. 1984;133:1710–5.
36. Thenappan A, Shukla V, Abdul Khalek FJ, Li Y, Shetty K, Liu P, et al. Loss of transforming growth factor beta adaptor protein beta-2 spectrin leads to delayed liver regeneration in mice. Hepatology. 2011;53:1641–50.
37. Jungermann K, Katz N. Functional specialization of different hepatocyte populations. Physiol Rev. 1989;69:708–64.
38. Halpern KB, Shenhav R, Matcovitch-Natan O, Toth B, Lemze D, Golan M, et al. Single-cell spatial reconstruction reveals global division of labour in the mammalian liver. Nature. 2017;542:352–6.
39. Maglich JM, Sluder A, Guan X, Shi Y, McKee DD, Carrick K, et al. Comparison of complete nuclear receptor sets from the human, *Caenorhabditis elegans* and *Drosophila* genomes. Genome Biol. 2001;2:RESEARCH0029.
40. Teng S, Jekerle V, Piquette-Miller M. Induction of ABCC3 (MRP3) by pregnane X receptor activators. Drug Metab Dispos. 2003;31:1296–9.
41. Chen W, Xiao Y, Cheng Y, Chen J, Chen J, Jiang K, et al. Pharmacokinetic differences of mifepristone between sexes in animals. J Pharm Biomed Anal. 2018;154:108–15.
42. Zhao B, Wei X, Li W, Udan RS, Yang Q, Kim J, et al. Inactivation of YAP oncoprotein by the Hippo pathway is involved in cell contact inhibition and tissue growth control. Genes Dev. 2007;21:2747–61.
43. Yu FX, Guan KL. The Hippo pathway: regulators and regulations. Genes Dev. 2013;27:355–71.
44. Kawana K, Ikuta T, Kobayashi Y, Gotoh O, Takeda K, Kawajiri K. Molecular mechanism of nuclear translocation of an orphan nuclear receptor, SXR. Mol Pharmacol. 2003;63:524–31.
45. Klaunig JE, Xu Y, Isenberg JS, Bachowski S, Kolaja KL, Jiang J, et al. The role of oxidative stress in chemical carcinogenesis. Environ Health Perspect. 1998;106 (Suppl 1):289–95.
46. Williams GM, Iatropoulos MJ. Alteration of liver cell function and proliferation: differentiation between adaptation and toxicity. Toxicol Pathol. 2002;30:41–53.
47. Sinz MW. Evaluation of pregnane X receptor (PXR)-mediated CYP3A4 drug-drug interactions in drug development. Drug Metab Rev. 2013;45:3–14.
48. Hedrich WD, Hassan HE, Wang H. Insights into CYP2B6-mediated drug-drug interactions. Acta Pharm Sin B. 2016;6:413–25.
49. Rulcova A, Prokopova I, Krausova L, Bitman M, Vrzal R, Dvorak Z, et al. Stereoselective interactions of warfarin enantiomers with the pregnane X nuclear receptor in gene regulation of major drug-metabolizing cytochrome P450 enzymes. J Thromb Haemost. 2010;8:2708–17.